Functional Links Between Aβ Toxicity, Endocytic Trafficking, and Alzheimer's Disease Risk Factors in Yeast

Sebastian Treusch *et al.*

Science **334**, 1241 (2011);
DOI: 10.1126/science.1213210

Science (print ISSN 0036-8075; online ISSN 1095-9203) is published weekly, except the last week in December, by the American Association for the Advancement of Science, 1200 New York Avenue NW, Washington, DC 20005.

Functional Links Between Aβ Toxicity, Endocytic Trafficking, and Alzheimer's Disease Risk Factors in Yeast

Sebastian Treusch,[1,2] Shusei Hamamichi,[1,3] Jessica L. Goodman,[1] Kent E. S. Matlack,[1,2] Chee Yeun Chung,[1] Valeriya Baru,[1,2] Joshua M. Shulman,[4,5] Antonio Parrado,[6] Brooke J. Bevis,[1] Julie S. Valastyan,[1,2] Haesun Han,[1] Malin Lindhagen-Persson,[7] Eric M. Reiman,[8,9] Denis A. Evans,[10] David A. Bennett,[11] Anders Olofsson,[7] Philip L. DeJager,[4,5] Rudolph E. Tanzi,[6] Kim A. Caldwell,[3] Guy A. Caldwell,[3] Susan Lindquist[1,2]*

Aβ (beta-amyloid peptide) is an important contributor to Alzheimer's disease (AD). We modeled Aβ toxicity in yeast by directing the peptide to the secretory pathway. A genome-wide screen for toxicity modifiers identified the yeast homolog of phosphatidylinositol binding clathrin assembly protein (*PICALM*) and other endocytic factors connected to AD whose relationship to Aβ was previously unknown. The factors identified in yeast modified Aβ toxicity in glutamatergic neurons of *Caenorhabditis elegans* and in primary rat cortical neurons. In yeast, Aβ impaired the endocytic trafficking of a plasma membrane receptor, which was ameliorated by endocytic pathway factors identified in the yeast screen. Thus, links between Aβ, endocytosis, and human AD risk factors can be ascertained with yeast as a model system.

Yeast cells lack the specialized processes of neuronal cells and the cell-cell communications that modulate neuropathology. However, the most fundamental features of eukaryotic cell biology evolved before the split between yeast and metazoans. Yeast studies of the cell cycle, DNA damage repair, and checkpoints produced pivotal advances in cancer biology (*1*). More recently, the conservation of protein-homeostasis networks, vesicular trafficking, mitochondrial biology, autophagy, and apoptosis facilitated the development of yeast models for protein-misfolding pathologies (*1*). When human diseases impinge on common features of eukaryotic cell biology, yeast's unequaled toolkit offers an attractive discovery platform, as established for multiple aspects of α-synuclein toxicity (*2*–*7*).

Here, we sought to create a yeast model of cellular toxicities elicited by the beta-amyloid (Aβ) peptide. According to the still hotly debated "amyloid cascade" hypothesis, Aβ is causal in both sporadic and familial Alzheimer's disease (AD) (*8*). The oligomeric forms of the peptide appear to be the most toxic (*9*–*12*). Similar toxic oligomers, formed by unrelated proteins but all recognized by the same conformation-specific antibody, are associated with other neurodegenerative diseases and with yeast prions (*13*, *14*). Thus, the toxicity of such oligomers is an ancient protein-folding problem.

In addition to Aβ, neurofibrillary tangles (NFTs) of tau, a microtubule-binding protein, are hallmarks of AD pathology (*15*). Aβ seems to act upstream of tau (*16*, *17*). Genetic AD risk factors are now being identified through genome-wide association studies (GWAS), but their relationship to Aβ is unknown.

A yeast model of Aβ toxicity. The most toxic form of Aβ, Aβ 1-42, is generated by proteolytic cleavage of APP, the transmembrane amyloid precursor protein (*18*, *19*). APP processing occurs in the secretory pathway, which releases Aβ into the trans-Golgi, endosomal compartments, and extracellular space. Aβ then interacts with the plasma membrane and is subject to endocytosis and further vesicular trafficking (*18*). To recapitulate this multicompartment trafficking in yeast, we fused an endoplasmic reticulum (ER) targeting signal to the N terminus of Aβ 1-42 (referred to as ssAβ 1-42). Without an ER retention signal, after cleavage of the signal sequence, Aβ 1-42 should simply transit through the secretory pathway to the plasma membrane (*20*). The yeast cell wall will restrain secreted peptides from diffusing into the culture medium, allowing Aβ to interact with the plasma membrane, undergo endocytosis, and thereby transit through endocytic compartments potentially relevant to AD (fig. S1A).

When expressed from a galactose-inducible (*GAL1*) promoter and a multicopy plasmid, ssAβ 1-42 decreased cell growth (Fig. 1A). When the same plasmid was used, Aβ 1-40 was less toxic, as were Pdi1 (an ER-resident protein), BPTI (a small protein commonly used to study secretion), and even BPTI^{C51A} [a variant that misfolds in the ER (*21*)] (Fig. 1A).

For genetic screens, strains with uniform stable ssAβ 1-42 expression were constructed by integrating tandem copies in the genome (fig. S1B). We targeted a locus where insertions have no deleterious consequences and selected strains that grew slowly upon galactose induction, but with no major increase in lethality (fig. S1C and table S1). The peptide produced was of the expected size for processed Aβ (fig. S1D), verified by mass spectrometry (fig. S1E). Localization to secretory compartments was confirmed by immunofluorescence (Fig. 1B).

When lysates were not subjected to boiling, which disrupts oligomeric species, we detected Aβ oligomers on Bis-Tris gels (fig. S1D). These forms reacted more strongly with the antibody NAB61, which preferentially recognizes toxic Aβ oligomers in AD patients (Fig. 1C) (*10*). These species disappeared upon boiling in lithium dodecyl sulfate buffer. Assaying lysates by size-exclusion chromatography with a monoclonal immunoglobulin M (IgM) antibody specific for Aβ oligomers detected a broad range of oligomeric species (Fig. 1D and fig. S1F) (*22*). Eliminating preparation artifacts, these were not seen when purified monomeric Aβ peptide was added to control cultures before lysis (Fig. 1D). In strains that produced the same amounts of Aβ 1-40 and 1-42 monomer after boiling (fig. S1G), oligomers were much more abundant for Aβ 1-42 before boiling (Fig. 1E). Thus, oligomeric Aβ forms contribute to toxicity in yeast, as in neurons.

Screen for genetic modifiers of Aβ toxicity. We transformed a screening strain with an overexpression library of 5532 full-length open reading frames (ORFs) (~90% of yeast ORFs) under control of the same promoter used for ssAβ 1-42 (fig. S2A). Individual transformants were arrayed in media that prevented induction of either ssAβ 1-42 or the library constructs, then plated (four replicates each) onto several types of inducing media, chosen to support different levels of mitochondrial respiration (fig. S2B and table S2) (*23*). Intermediate levels of Aβ toxicity enabled the identification of enhancers and suppressors in the same screen (fig. S1B and table S2) (*23*). Genes that decreased or increased growth (fig. S2B) were retested in an independently derived screening strain. Secondary screens eliminated genes that simply altered expression of Aβ from the *GAL1* promoter (fig. S3) or growth in the absence of Aβ.

[1]Whitehead Institute for Biomedical Research, Cambridge, MA 02142, USA. [2]Howard Hughes Medical Institute, Department of Biology, Massachusetts Institute of Technology, Cambridge, MA 02139, USA. [3]Department of Biological Sciences, The University of Alabama, Tuscaloosa, AL 35487, USA. [4]Program in Translational NeuroPsychiatric Genomics, Institute for the Neurosciences, Departments of Neurology and Psychiatry, Brigham and Women's Hospital and Harvard Medical School, Boston, MA 02115, USA. [5]Program in Medical and Population Genetics, Broad Institute, Cambridge, MA 02142, USA. [6]Genetics and Aging Research Unit, Massachusetts General Hospital, Harvard Medical School, Charlestown, MA 02129, USA. [7]Department of Medical Biochemistry and Biophysics, Umea University, Umea, Sweden. [8]Neurogenomics Division, Translational Genomics Research Institute and Arizona Alzheimer's Consortium, Phoenix, AZ 85004, USA. [9]Banner Alzheimer's Institute and Department of Psychiatry, University of Arizona, Phoenix, AZ 85006, USA. [10]Rush Institute for Healthy Aging, Department of Internal Medicine, Rush University Medical Center, Chicago, IL 60612, USA. [11]Rush Alzheimer's Disease Center, Department of Neurological Sciences, Rush University Medical Center, Chicago, IL 60612, USA.

*To whom correspondence should be addressed. E-mail: lindquist_admin@wi.mit.edu

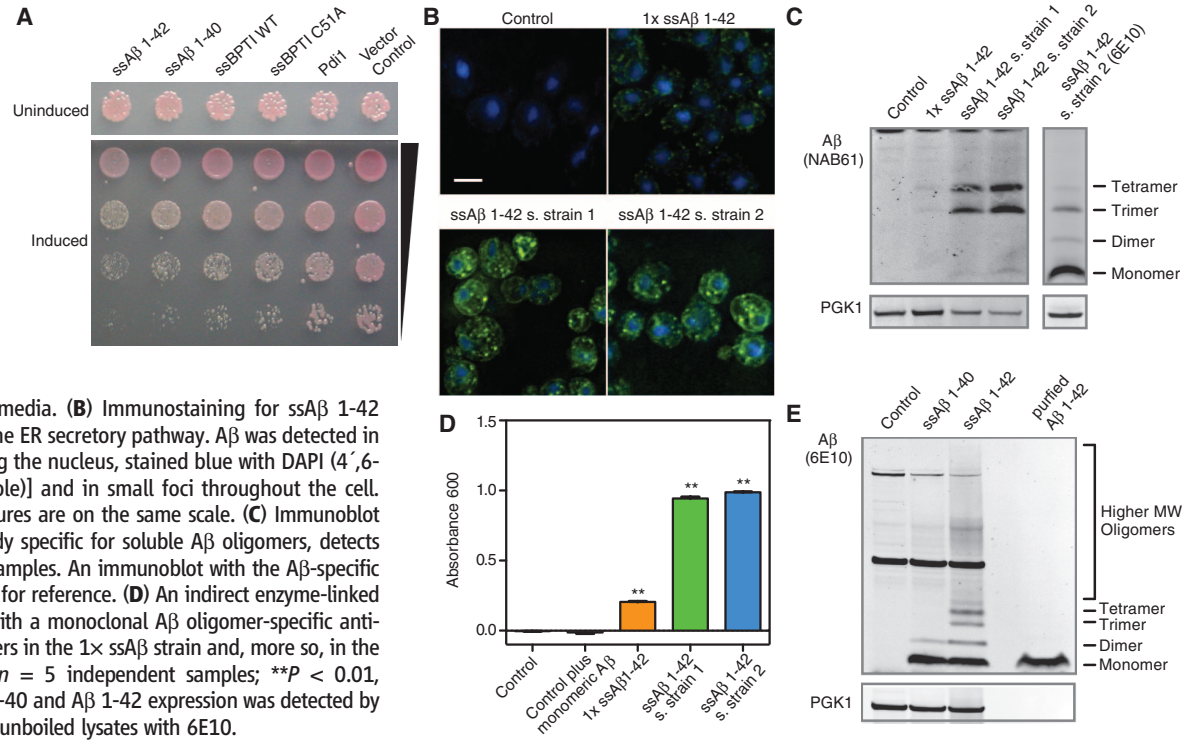

Fig. 1. Expression of Aβ in the yeast secretory pathway. (**A**) Comparison of ssAβ 1-42 toxicity with ssAβ 1-40, ssBPTI [wild-type (WT) and C51A], and Pdi1. Proteins were expressed with the inducible *GAL1* promoter and a high–copy number plasmid. Strains carrying the plasmids were serially diluted and spotted on inducing (galactose) and noninducing (glucose) media. (**B**) Immunostaining for ssAβ 1-42 reveals localization to the ER secretory pathway. Aβ was detected in the ER [ring surrounding the nucleus, stained blue with DAPI (4′,6-diamidino-2-phenylindole)] and in small foci throughout the cell. Scale bar: 5 μm. All figures are on the same scale. (**C**) Immunoblot with NAB61, an antibody specific for soluble Aβ oligomers, detects oligomers in unboiled samples. An immunoblot with the Aβ-specific antibody 6E10 is shown for reference. (**D**) An indirect enzyme-linked immunosorbent assay with a monoclonal Aβ oligomer-specific antibody detects Aβ oligomers in the 1× ssAβ strain and, more so, in the two screening strains (n = 5 independent samples; $^{**}P < 0.01$, Dunnett's test). (**E**) Aβ 1-40 and Aβ 1-42 expression was detected by immunoblot analysis of unboiled lysates with 6E10.

We identified 23 suppressors and 17 enhancers (table S2). Only a few modifiers were strongly affected by the state of respiration (table S2). The screen hits comprised a wide range of cellular functions. Numerous hits had sequence similarity to human genes, and 12 had very clear human homologs (determined by HomoloGene or by analogous functionality (*SLA1*/*SH3KBP1*) (*24*)) (Table 1). We focused further analysis on these.

Three of these 12 genes had functions related to clathrin-mediated endocytosis (*YAP1802*, *INP52*, *SLA1*; $P = 3.89 \times 10^{-4}$) and seven were functionally associated with the cytoskeleton (*YAP1802*, *INP52*, *SLA1*, *CRM1*, *GRR1*, *KEM1*, and *RTS1*; $P = 6.06 \times 10^{-8}$). None were identified in our previous screen for modifiers of α-syn toxicity (*5*, *7*), establishing their specificity for the type of toxicity caused by Aβ 1-42.

Modifiers of Aβ toxicity are associated with AD susceptibility. Several human homologs of our yeast hits had connections to human AD risk factors, particularly those involved in clathrin-mediated endocytosis (Table 1). The human homolog of yeast *YAP1802*, *PICALM*, is one of the most highly confirmed risk factors for sporadic AD (*25*, *26*). Another AD risk factor, *BIN1* (*27*), is involved in synaptic vesicle endocytosis and is believed to interact with synaptojanin, the human homolog of yeast *INP52* (*28*). The functional homolog of yeast *SLA1*, *SH3KBP1* (*29*), directly interacts with the risk factor *CD2AP* (*30*, *31*). *CD2AP* links endocytosis to cytoskeletal dynamics and our other major class of screen hits.

To assess the potential clinical relevance of other screen hits with highly conserved human homologs, we examined association with AD susceptibility using data from a published family-based GWAS (*32*, *33*). Using a family-based association test, we discovered a suggestive association of *XPO1* (*CRM1* homolog, rs6545886, $P = 0.003$) with AD susceptibility (*23*) (table S3).

Next, we leveraged genotyping with extensive clinical and pathological data from two large epidemiological studies of aging, cognition, and AD (*23*, *34*, *35*) (tables S4 to S7). Using a quantitative summary measure of global AD pathologic burden available in these cohorts, counting

Table 1. Genes that modify Aβ toxicity. Yeast genes with clear nematode and human homologs were identified in an unbiased screen of 5532 single-copy plasmids carrying yeast ORFs under the control of the *GAL1* promoter in three independent screens in three inducing medias (*23*).

Yeast Aβ suppressors	Cellular function	*C. elegans* homolog	Human homolog	Connection of human homologs to AD risk
YAP1802	Endocytosis	*unc-11**	*PICALM*	Validated risk factor†‡
INP52	Endocytosis	*unc-26**	*SYNJ1*	Interacts with validated risk factor *BIN1* (*28*)
SLA1	Endocytosis	*Y44E3A.4**	*SH3KBP1*	Interacts with validated risk factor *CD2AP* (*29*)
RTS1	Phosphatase regulation	*pptr-2**	*PPP2R5C*	
ADE12	Adenylosuccinate synthesis	*C37H5.6b**	*ADSSL1*	Potential risk factor, this study§
CRM1	Nuclear protein export	*xpo-1**	*XPO1*	Potential risk factor, this study‡
GRR1	Ubiquitination	*C02F5.7*	*FBXL2*	
VPS9	Vesicle transport	*rabx-5*	*RABGEF1*	Potential risk factor, this study§
Yeast Aβ enhancers				
PBS2	Osmotic stress response	*mkk-4**	*MAP2K4*	Activated by Aβ oligomers in cortical neurons (*37*)
KEM1	RNA processing	*xrn-1*	*XRN1*	
MVP1	Vacuolar sorting	*lst-4*	*SNX8*	
PMT2	Mannosylation	—	*POMT2*	

*Genes tested in the *C. elegans* model. †Table S3. ‡Table S6. §Table S7.

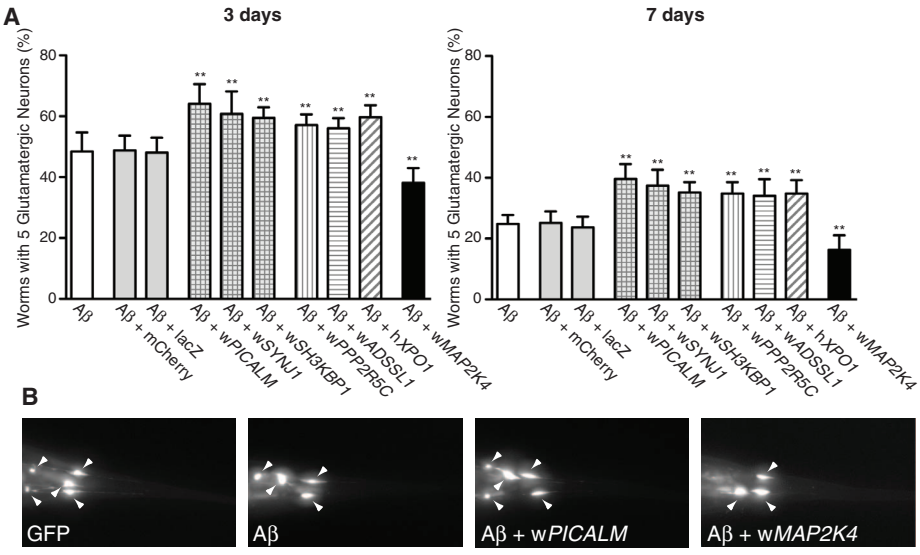

Fig. 2. Hits from the yeast screen modify the toxicity of Aβ in *C. elegans* glutamatergic neurons in the same direction as in yeast. (**A**) A new animal model of Aβ toxicity. Aβ 1-42, carrying a signal sequence targeting it to the secretory compartment, was expressed in glutamatergic neurons that also expressed GFP. Neuronal death increased from 50% at day 3 to 75% at day 7, establishing that this worm model exhibits age-dependent neurodegeneration. Control genes mCherry and LacZ had no effect on Aβ-induced neurodegeneration. Measurements are relative to the number of neurons found in WT worms expressing only GFP. Bar patterns indicate distinct functional categories (crosshatches for endocytic genes). The genetic modifiers tested influenced Aβ toxicity significantly (**$P < 0.05$, Student's t test, error bars indicate standard deviations). *XPO1* was derived from human cDNA. For each worm (w) or human (h) gene, three transgenic lines were established and 90 worms examined for each. (**B**) Representative examples of worms scored in Fig. 2A at the third day of development. Arrowheads indicate neuronal cell bodies, marked by transgenic expression of GFP.

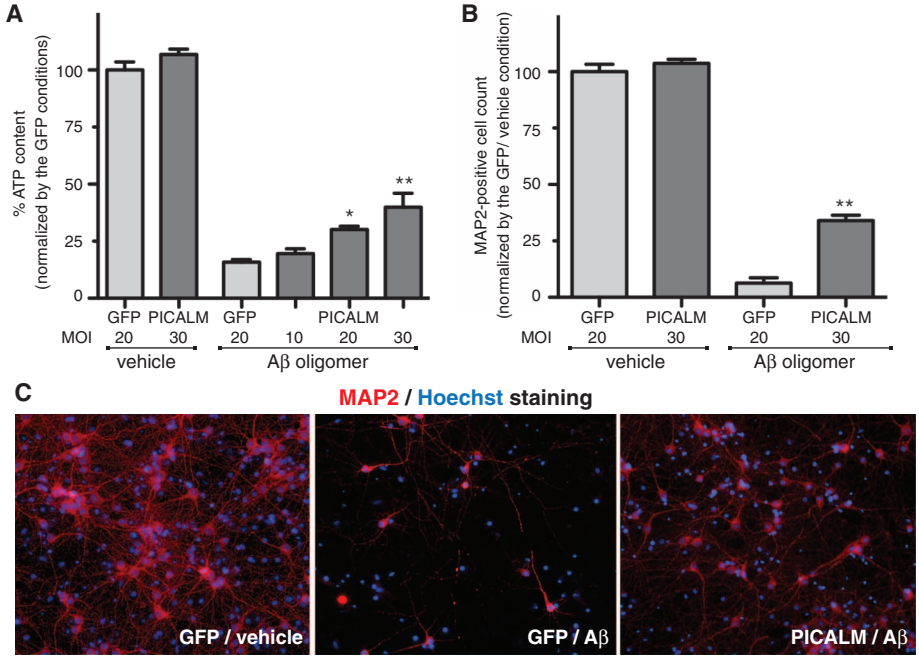

Fig. 3. *PICALM* protects cultured rat cortical neurons from exogenously applied Aβ oligomers. Cortical neuron cultures prepared from rat embryos at embryonic day 18 were cultured for 5 days, transduced, cultured for 13 days, and then incubated for 20 hours with 750 nM soluble Aβ oligomers prepared from synthetic peptide (*23*). Infection with a *PICALM* lentiviral construct diminished toxicity in a dose-dependent, statistically significant manner. Cell viability was assessed by both adenosine 5′-triphosphate (ATP) content (**A**) and MAP2-positive cell counting (**B** and **C**). Data are representative of three independent experiments and shown as mean ± SEM [*$P < 0.05$; **$P < 0.01$, Dunnett's test (A) and two-tailed t test (B)].

both amyloid plaques and NFTs, we found that two additional loci identified by our yeast screen, *ADSSL1* (*ADE12* homolog, rs1128880, $P = 0.001$) and *RABGEF1* (*VPS9* homolog, rs17566701, $P = 0.002$), showed evidence of association with AD neuropathology (table S7). Both loci also harbored suggestive association signals with episodic memory decline (table S6). Thus, our yeast screen connects multiple human AD risk factors, and suggested risk factors, to Aβ toxicity.

***C. elegans* model of Aβ toxicity.** To directly test our modifiers for effects on Aβ toxicity in neurons, we created a transgenic *C. elegans* model that expressed Aβ 1-42 in glutamatergic neurons, a neuronal subtype particularly vulnerable in AD. [A previous model expressed Aβ in body-wall muscles (*36*).] We used the *eat-4* promoter, which regulates expression of the BNPI glutamate transporter and, again, targeted Aβ to the secretory pathway (*36*). The Aβ transgene was integrated into chromosomal DNA to ensure the same Aβ 1-42 expression levels in all animals.

C. elegans has highly stereotyped cell lineages. Wild-type worms invariably have five glutamatergic neurons in their tails, which we visualized with *eat-4*–regulated green fluorescent protein (GFP). Crossing worms expressing ssAβ to worms carrying this reporter resulted in the loss of GFP-marked glutamatergic neurons in an age-related manner; at day 3 only 48% of worms had five intact glutamatergic neurons, and at day 7 only 25% did (Fig. 2A).

To test the effects of our screen hits (Table 1), we established three independent transgenic worm lines for each gene, again expressing the protein from the *eat-4* promoter. Unrelated control proteins mCherry and LacZ had no effect on Aβ toxicity. All three *C. elegans* homologs of the genes involved in clathrin-mediated endocytosis—*unc-11*, *unc-26*, and *Y44E3A.4*—increased the percentage of worms with five intact glutamatergic neurons (Fig. 2).

Finally, we tested four hits—three suppressors and one enhancer—involved in a diverse array of pathways. The yeast *RTS1* gene encodes a phosphatase regulatory subunit that controls several stress-response pathways. The *ADE12* gene product catalyzes the first step in the synthesis of adenosine monophosphate from inosine 5-monophosphate. The *C. elegans* homologs of each gene suppressed the Aβ-induced loss of glutamatergic neurons (Fig. 2A). We were unable to clone the worm homologs of *GRR1*, *VPS9*, or *CRM1*. However, *CRM1* encodes a highly conserved nuclear export receptor. Expression of a *CRM1* human homolog, *XPO1*, protected nematode glutamatergic neurons from Aβ (Fig. 2A). *PBS2/MAP2K4*, a mitogen-activated protein (MAP) kinase involved in stress responses, increased neuronal loss (Fig. 2).

The effect of each gene was statistically significant ($P < 0.05$) for both the modest neuronal toxicity evinced at 3 days and the more severe toxicity at 7 days. Notably, the modifiers did not alter the levels of Aβ mRNA, as tested by

semiquantitative reverse transcriptase–polymerase chain reaction (fig. S5). Thus, every gene we tested in *C. elegans* glutamatergic neurons modified Aβ toxicity in the same direction (suppression versus enhancement) as they did in yeast.

***PICALM* suppresses the toxicity of soluble Aβ oligomers with rat cortical neurons.** *PICALM* is one of the most highly validated AD risk factors, and its efficacy in our yeast and nematode models strongly suggests that it alters Aβ toxicity. Modeling this in cultured mammalian neurons is not trivial, because any Aβ peptide expressed in the secretory pathway would simply diffuse away from the cell. Exogenously applied, preformed oligomeric Aβ species are often used to model toxicity (*13*, *37*), but their relevance is highly debated. We reasoned that a positive result for the highly validated AD risk factor *PICALM* might not only validate this assay but confirm the role of *PICALM* in Aβ detoxification.

We analyzed cortical neurons, a neuronal population particularly relevant to AD. Embryos from female rats with timed pregnancies were harvested at 18 days of gestation. Cortices dissected from these embryos were dissociated, plated, and cultured for up to 21 days (*23*). The production of toxic Aβ oligomers is notoriously variable. We prepared oligomers according to several published methods, characterized them biochemically, and tested them for producing consistent levels of toxicity in our cortical neuronal preparations (Fig. 3 and figs. S6 and S7). The loss of toxicity when the same samples were allowed to form Aβ fibers (fig. S6, A and C) confirmed the importance of the oligomeric species (fig. S6D).

Next, we infected neurons with lentiviruses engineered to express GFP or *PICALM*. When Aβ oligomers were added to these neurons, GFP had no effect, but *PICALM* partially rescued the cells from Aβ-induced cell death in a dose-dependent manner (Fig. 3). Rescue was significant whether assayed by cellular ATP content (Fig. 3A) or by counting the number of MAP2-positive neurons (Fig. 3, B and C). As previously described for midbrain neurons (*7*), we found that *RAB1* protected cortical neurons from α-syn toxicity when this protein was expressed intracellularly by viral transfection. However, *RAB1* was ineffective against Aβ oligomers, confirming the specificity of *PICALM* for the type of toxicity caused by Aβ oligomers (fig. S7).

Effect of Aβ on endocytosis and trafficking. The role of *PICALM* in AD is unknown, but it has been postulated to affect disease by modifying APP trafficking (*25*). However, our experiments in yeast, nematode, and rat neurons clearly establish *PICALM* as a modifier of Aβ toxicity itself. To investigate the mechanism by which *PICALM* and the other modifiers affect clathrin-mediated endocytosis, we returned to yeast.

One possibility is that clathrin-mediated endocytosis modulates Aβ toxicity simply by shunting toxic Aβ species to the lysosomal-vacuolar system for degradation. However, immunoblotting of yeast lysates indicated that these modifiers had little effect on Aβ levels (fig. S4). Alternatively, if Aβ specifically perturbs endocytic homeostasis, up-regulation of this pathway might ameliorate the defect.

To determine if Aβ altered clathrin distributions, we used a strain in which endogenous clathrin light chain 1 (Clc1) was tagged with GFP, a fully functional fusion. A control strain exhibited the expected distribution of Clc1-GFP foci (*38*). Aβ perturbed clathrin localization, increasing both the number and brightness of foci, but decreasing their average size (Fig. 4A).

Such a pattern might indicate a defect in clathrin-mediated secretion as well as in endocytosis. To test effects of Aβ on secretion, we used a halo assay for secretion of the α-factor mating pheromone. As a control, we also tested the effects of α-syn expression, which produces a strong defect in secretion (*7*) (Fig. 4B). Unlike α-syn, Aβ did not inhibit secretion (Fig. 4B).

To assess the effect of Aβ on clathrin-mediated endocytosis specifically, we examined the well-characterized substrate Ste3, a member of the highly conserved G protein–coupled receptor family. Ste3 is targeted to the plasma membrane. In the absence of its ligand, the yeast mating factor, it is constitutively endocytosed and degraded in the vacuole (*39*). As expected, a Ste3-YFP (yellow fluorescent protein) fusion was primarily localized to the vacuole in a control strain (Fig. 4C). In Aβ-expressing strains, endocytic trafficking of Ste3-YFP was profoundly perturbed, and the protein was localized to numerous foci (*23*) (Fig. 4C). Aβ expression resulted in a reduction of vacuolar organelle size without a disruption in morphology, consistent with reduced delivery of cargo to this organelle. Finally, we tested the effects of the three Aβ toxicity suppressors that function in endocytic trafficking—*YAP1802*, *INP52*, and *SLA1*. Each partially reversed the defect in Ste3-YFP trafficking (Fig. 4C).

Conclusions and perspectives. Our yeast model allowed us to conduct an unbiased screen of an entire genome for modifiers of Aβ toxicity. The emergence of three different genes involved in the process of clathrin-mediated endocytosis from nearly 6000 tested ORFs confirms that the Aβ peptide in our model is trafficking through the secretory compartments as expected. Moreover, the ability of endocytic genes to rescue Aβ toxicity, together with the effects of Aβ on clathrin localization and the trafficking of a G protein–coupled receptor, establish that within these highly diverse organisms, clathrin-mediated endocytosis is a critical point of vulnerability to Aβ.

Aβ oligomers have been reported to increase endocytosis in cultured cells (*40*), and human-induced neuronal cells derived from the fibroblasts of AD patients exhibit defects in endocytosis (*41*). Mechanistically, in our Aβ-expressing cells, the increased number of clathrin foci, the internalized foci of Ste3, and the effects of genetic modifiers on vacuolar localization all suggest that Aβ affects this pathway by interfering with the ability of endocytosed transmembrane receptors to reach their proper destinations.

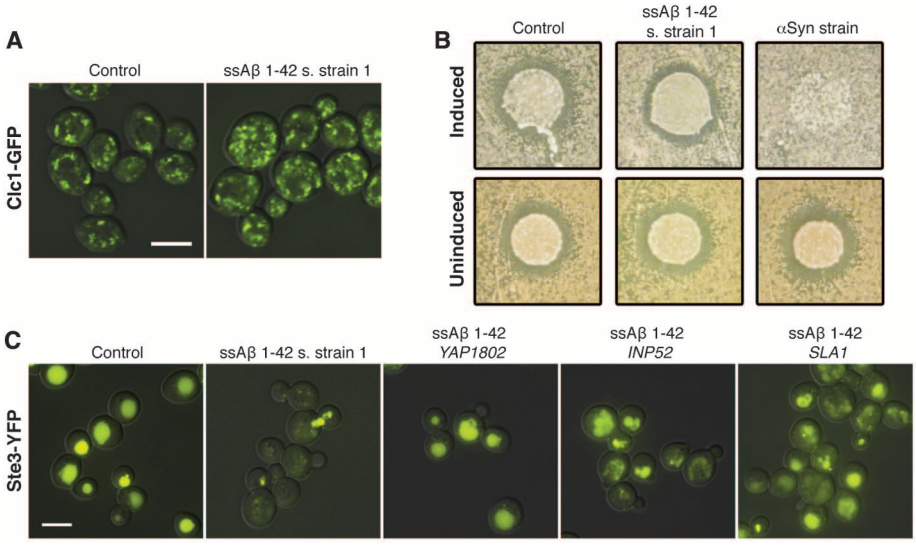

Fig. 4. Aβ causes defects in endocytosis and receptor protein trafficking. (**A**) In a yeast strain with GFP-tagged clathrin light chain 1 (Clc1-GFP), ssAβ 1-42 caused an increase in Clc1-GFP foci. (**B**) A halo assay, which measures secretion of the α-factor pheromone, was used to assess secretion. In the screening strain, ssAβ 1-42 diminished growth but did not reduce secretion compared to the vector control. In contrast, a strain expressing α-syn, which impedes ER-Golgi trafficking, exhibits a strong defect in secretion. (**C**) Aβ 1-42 caused a defect in the normal trafficking of Ste3 to the vacuole. A Ste3-YFP fusion is normally trafficked to the vacuole. Aβ-expressing cells showed accumulation of Ste3-YFP in cytoplasmic foci. Coexpression of *YAP1802*, *INP52*, and *SLA1* partially restored Ste3-YFP trafficking to the vacuole. A constitutively expressed gene encoding Ste3-YFP was integrated in the genome of the control and screening strain. Scale bars: 5 μm. All images are on the same scale.

PICALM, as well as two genes whose protein products (*BIN1* and *CD2AP*) interact with hits from our screen, are AD risk factors. Given the diversity of pathologies, however, their connection to Aβ toxicity was unknown. Our work in yeast, nematodes, and rat cortical neurons clearly places these factors within the Aβ cascade, linking Aβ to the genetics of sporadic AD.

Neurons are particularly vulnerable to perturbations in the homeostasis of endocytosis, because they must constantly recycle both neurotransmitters and their receptors (*42*). Aβ interacts with, and alters signaling by, a variety of neuronal receptors (*43*). We propose that the conformational flexibility of these oligomers allows them to interact rather promiscuously with conformationally flexible unliganded receptors, which, in turn, disrupts endocytic homeostasis.

Our yeast screen also identified seven conserved genes functionally associated with the cytoskeleton. Because yeasts do not express tau, our findings may indicate that the connection between Aβ toxicity and the cytoskeleton is more deeply rooted than tau alone, probably involving clathrin-mediated endocytosis. In analyzing human GWAS data we also uncovered suggestive associations between AD and three other genes—*XPO1*, *ADSSL1*, and *RABGEF1*—and confirmed their Aβ relationships in yeast and nematode.

The treatments available for AD are few and their efficacy limited. Determining how best to rescue neuronal function in the context of the whole brain is a problem of staggering proportions. Our yeast model provides a tool for identifying genetic leads, investigating their mechanisms of action, and screening for genetic and small-molecule modifiers of this devastating and etiologically complex disease.

References and Notes

1. V. Khurana, S. Lindquist, *Nat. Rev. Neurosci.* **11**, 436 (2010).
2. T. F. Outeiro, S. Lindquist, *Science* **302**, 1772 (2003).
3. N. Thayanidhi *et al.*, *Mol. Biol. Cell* **21**, 1850 (2010).
4. A. R. Winslow *et al.*, *J. Cell Biol.* **190**, 1023 (2010).
5. A. D. Gitler *et al.*, *Nat. Genet.* **41**, 308 (2009).
6. L. J. Su *et al.*, *Dis Model Mech* **3**, 194 (2010).
7. A. A. Cooper *et al.*, *Science* **313**, 324 (2006).
8. J. Hardy, D. J. Selkoe, *Science* **297**, 353 (2002).
9. M. Knobloch, U. Konietzko, D. C. Krebs, R. M. Nitsch, *Neurobiol. Aging* **28**, 1297 (2007).
10. E. B. Lee *et al.*, *J. Biol. Chem.* **281**, 4292 (2006).
11. G. M. Shankar *et al.*, *Nat. Med.* **14**, 837 (2008).
12. D. M. Walsh, B. P. Tseng, R. E. Rydel, M. B. Podlisny, D. J. Selkoe, *Biochemistry* **39**, 10831 (2000).
13. R. Kayed *et al.*, *Science* **300**, 486 (2003).
14. J. Shorter, S. Lindquist, *Science* **304**, 1793 (2004).
15. F. M. LaFerla, *Biochem. Soc. Trans.* **38**, 993 (2010).
16. L. M. Ittner *et al.*, *Cell* **142**, 387 (2010).
17. E. D. Roberson *et al.*, *Science* **316**, 750 (2007).
18. G. Thinakaran, E. H. Koo, *J. Biol. Chem.* **283**, 29615 (2008).
19. D. J. Selkoe, M. S. Wolfe, *Cell* **131**, 215 (2007).
20. H. R. Pelham, *Annu. Rev. Cell Biol.* **5**, 1 (1989).
21. J. M. Kowalski, R. N. Parekh, K. D. Wittrup, *Biochemistry* **37**, 1264 (1998).
22. M. Lindhagen-Persson, K. Brännström, M. Vestling, M. Steinitz, A. Olofsson, *PLoS ONE* **5**, e13928 (2010).
23. Supporting material is available on *Science* Online.
24. S. D. Stamenova, R. Dunn, A. S. Adler, L. Hicke, *J. Biol. Chem.* **279**, 16017 (2004).
25. D. Harold *et al.*, *Nat. Genet.* **41**, 1088 (2009).
26. J. C. Lambert *et al.*; European Alzheimer's Disease Initiative Investigators, *Nat. Genet.* **41**, 1094 (2009).
27. S. Seshadri *et al.*, *JAMA* **303**, 1832 (2010).
28. A. R. Ramjaun, K. D. Micheva, I. Bouchelet, P. S. McPherson, *J. Biol. Chem.* **272**, 16700 (1997).
29. G. Gaidos, S. Soni, D. J. Oswald, P. A. Toselli, K. H. Kirsch, *J. Cell Sci.* **120**, 2366 (2007).
30. P. Hollingworth *et al.*; Alzheimer's Disease Neuroimaging Initiative; CHARGE consortium; EADI1 consortium, *Nat. Genet.* **43**, 429 (2011).
31. A. C. Naj *et al.*, *Nat. Genet.* **43**, 436 (2011).
32. L. Bertram *et al.*, *Am. J. Hum. Genet.* **83**, 623 (2008).
33. D. Blacker *et al.*, *Neurology* **48**, 139 (1997).
34. D. A. Bennett, P. L. De Jager, S. E. Leurgans, J. A. Schneider, *Neurology* **72**, 1495 (2009).
35. J. M. Shulman *et al.*, *PLoS ONE* **5**, e11244 (2010).
36. C. D. Link, *Proc. Natl. Acad. Sci. U.S.A.* **92**, 9368 (1995).
37. D. Bozyczko-Coyne *et al.*, *J. Neurochem.* **77**, 849 (2001).
38. Y. Sun, S. Carroll, M. Kaksonen, J. Y. Toshima, D. G. Drubin, *J. Cell Biol.* **177**, 355 (2007).
39. L. Maldonado-Báez *et al.*, *Mol. Biol. Cell* **19**, 2936 (2008).
40. A. J. Miñano-Molina *et al.*, *J. Biol. Chem.* **286**, 27311 (2011).
41. L. Qiang *et al.*, *Cell* **146**, 359 (2011).
42. N. Jung, V. Haucke, *Traffic* **8**, 1129 (2007).
43. Y. Verdier, M. Zarándi, B. Penke, *J. Pept. Sci.* **10**, 229 (2004).

Acknowledgments: We thank L. Chibnik, B. Keenan, and D. Ng for helpful discussions; D. Wittrup, V. Lee, M. Vidal, and C. Link for materials; and J. Corneveaux, M. Huentelman, and other Translational Genomics investigators for assistance with the human study cohorts and participants in the Religious Orders Study and the Rush Memory and Aging Project. This work was supported by a Howard Hughes Medical Institute Collaborative Innovation Award; National Research Service Award fellowship F32 NS067782-02; the Cure Alzheimer's Fund; NIH grants K08AG034290, P30AG10161, R01AG15819, and R01AG17917; the Kempe foundation; and Alzheimerfonden. This paper is dedicated to Nell Matheney, Zhao Xindi, Rochelle Glatt, Matyas Topolszki, their families, and the countless other victims of Alzheimer's disease.

Supporting Online Material

www.sciencemag.org/cgi/content/full/science.1213210/DC1
Materials and Methods
Figs. S1 to S7
Tables S1 to S7
References (*44*–*57*)

26 August 2011; accepted 18 October 2011
Published online 27 October 2011;
10.1126/science.1213210

Detection of Pristine Gas Two Billion Years After the Big Bang

Michele Fumagalli,[1]* John M. O'Meara,[2] J. Xavier Prochaska[3]

In the current cosmological model, only the three lightest elements were created in the first few minutes after the Big Bang; all other elements were produced later in stars. To date, however, heavy elements have been observed in all astrophysical environments. We report the detection of two gas clouds with no discernible elements heavier than hydrogen. These systems exhibit the lowest heavy-element abundance in the early universe, and thus are potential fuel for the most metal-poor halo stars. The detection of deuterium in one system at the level predicted by primordial nucleosynthesis provides a direct confirmation of the standard cosmological model. The composition of these clouds further implies that the transport of heavy elements from galaxies to their surroundings is highly inhomogeneous.

In modern cosmological theory, the light elements and their isotopes were produced during the first few minutes after the Big Bang, when the universe cooled during expansion from temperatures $T \sim 10^9$ K to below $\sim 4 \times 10^8$ K. In this brief epoch, termed Big Bang nucleosynthesis (BBN), deuterium (D), ^{3}He, ^{4}He, and ^{7}Li were synthesized with an abundance ratio relative to hydrogen (H) that was sensitive to the cosmic density of ordinary matter (i.e., the baryon density $\Omega_{b,0}$). BBN theory also predicts that there was negligible production of the heavy elements with abundance ratios X/H $< 10^{-10}$, because the physical conditions now typical of stellar interiors did not yet exist (*1*).

The analysis of gas observed in absorption along the lines of sight to high-redshift quasars, distant galaxies that host supermassive black holes, is a powerful probe of the BBN yields. Particular attention has been given to D, partly because of observational convenience, but also because the D/H abundance ratio is very sensitive to $\Omega_{b,0}$. For quasar sight lines, the measured $\log(\mathrm{D/H}) = -4.55 \pm 0.03$ (*2*, *3*) translates into $\Omega_{b,0}h^2(\mathrm{BBN}) = 0.0213 \pm 0.0010$, which is fully consistent with the value inferred from the cosmic

[1]Department of Astronomy and Astrophysics, University of California, Santa Cruz, CA, USA. [2]Department of Chemistry and Physics, Saint Michael's College, Colchester, VT, USA. [3]University of California Observatories–Lick Observatory, University of California, Santa Cruz, CA, USA.

*To whom correspondence should be addressed. E-mail: mfumagalli@ucolick.org